JOURNAL OF MAGNETIC RESONANCE **124,** 97–103 (1997)
ARTICLE NO. MN967478

Selective Transient Heteronuclear Cross Relaxation in a Selectively $^{13}C^{\alpha}$-Labeled Peptide

PETER ALLARD,* JÜRI JARVET,† AND ASTRID GRÄSLUND†‡

*Center for Structural Biochemistry, Karolinska Institutet and the Royal Institute of Technology, NOVUM, S-141 57 Huddinge, Sweden; and †Department of Biophysics, Arrhenius Laboratories, Stockholm University, S-106 91 Stockholm, Sweden

Received July 15, 1996; revised September 3, 1996

A new pulse sequence for the direct measurement of heteronuclear cross-relaxation rates is presented. The pulse sequence uses proton detection of transient carbon magnetization with sensitivity-enhanced transfer of magnetization and pulsed field gradients for coherence selection and water suppression. The heteronuclear cross-relaxation rate is measured using either nonselective or selective inversion of all or particular protons. A technique for the suppression of spin diffusion is also applied. The pulse sequence is tested on a peptide with a selectively ^{13}C-labeled α-carbon. The directly measured rate is compared with and agrees well with the cross-relaxation rates as traditionally calculated from the steady-state NOE and carbon longitudinal-relaxation rate.

INTRODUCTION

The dynamics of biomolecules can be probed by the NMR relaxation rates of intrinsic reporter groups such as the heteronuclei ^{13}C and ^{15}N. The interaction constants of the dominating dipole–dipole and chemical-shift-anisotropy relaxation mechanisms are usually known and the distance between the heteronucleus and its neighboring proton is well defined. The relaxation rates of a heteronucleus–proton pair can be directly related to the parameters of molecular mobility. When using magnetic fields strengths on the order of 10 T, NMR relaxation is very sensitive to rotational diffusion of medium-sized proteins, which occurs in the nanosecond time region. From NMR relaxation experiments, is it possible to obtain a detailed description of molecular dynamics. Depending on the number and accuracy of relaxation rates measured, the experimental data can be analyzed either by using the model-free approach (*1, 2*) or by the spectral-density-mapping technique (*3*). In order to use the full potential of these methods, all relaxation rates must be determined without systematic bias and with high accuracy.

In a detailed NMR study of protein dynamics, a number of relaxation rates should be measured. One of the most frequently measured rates is the heteronuclear cross-relaxation rate σ between an α carbon and an α proton or between an amide nitrogen and an amide proton. This rate is sensitive to the difference of the spectral density at the frequencies $\omega_H + \omega_X$ and $\omega_H - \omega_X$ and probes the dynamics on the nanosecond time scale. The cross-relaxation rate is usually calculated indirectly from the measured heteronuclear steady-state NOE and the longitudinal-relaxation rate of the heteronucleus. Here we present a direct and selective method for measuring the cross-relaxation rate between a heteronucleus and any of its neighboring protons. The basic idea of this experiment is the same as that described by Solomon (*4*). The sensitivity of the pulse sequence described here is increased by proton detection of the heteronucleus magnetization, which allows the method to be applied to samples at millimolar concentration. Water suppression is performed with pulsed field gradients. The selectivity with respect to different protons surrounding the heteronucleus is achieved by using a selective proton pulse. The protons of neighboring residues are usually distant in space and they do not contribute directly to the relaxation of the heteronucleus being studied. By selective inversion of the studied pair of spins in the middle of the mixing time, we could eliminate the effects of spin diffusion between spatially close protons. The method to quench effects of spin diffusion is similar to the approach described previously for XD-NOESY (*5*), SNOESY (*6*), and QUIET-NOESY (*7*) experiments.

We have previously mapped the spectral-density function $J(\omega)$, describing the $^{13}C^{\alpha}-{}^{1}H^{\alpha}$ vector dynamics of Leu^{10} in the 22-residue peptide hormone motilin, by using three polarizing fields 9.4, 11.7, and 14.1 T (*8*) and at several temperatures at one field, 9.4 T (*9*). The present study of selective cross relaxation was undertaken in order to test the accuracy of the reported $^{13}C^{\alpha}-{}^{1}H^{\alpha}$ cross-relaxation rates, which were previously calculated from the steady-state NOE and the carbon longitudinal-relaxation rate, and in addition to gain a better understanding of the influence from other protons on the α-carbon relaxation.

‡ To whom correspondence should be addressed.

1090-7807/97 $25.00

THEORY

The Solomon Equations for Two Spins

The spin-system dynamics was analyzed using a two-spin approximation as described in (*10*). The ^{13}C spin will be denoted by 1 and the ^{1}H spin by 2. The time dependence of the corresponding transient magnetizations M_1 and M_2 is described by the Solomon equations

$$\frac{dM_1}{dt} = -R_{11}(M_1 - M_1^{eq}) - \sigma_{12}(M_2 - M_2^{eq})$$

$$\frac{dM_2}{dt} = -\sigma_{21}(M_1 - M_1^{eq}) - R_{22}(M_2 - M_2^{eq}), \qquad [1]$$

where R_{ii} is the longitudinal-relaxation rate of spin i and σ_{ij} is the cross-relaxation rate between spins i and j. M_i^{eq} is the equilibrium magnetization of spin i. The general solution of Eq. [1] for the relative magnetization of spin 1 after a perturbation may be written

$$\frac{M_1}{M_1^{eq}} = 1 + \frac{C_1 e^{-\lambda_1 t} + C_2 e^{-\lambda_2 t}}{M_1^{eq}}, \qquad [2]$$

where λ_1 and λ_2 are roots of the characteristic equation

$$\lambda_{1,2} = \frac{1}{2} \times \{(R_{11} + R_{22}) \pm [(R_{11} - R_{22})^2 + 4\sigma_{12}\sigma_{21}]^{1/2}\}. \qquad [3]$$

Consider the case where at time $t = 0$, the magnetization of spin 2 has been inverted by applying a 180° pulse. After this pulse, the initial conditions are $M_1(t = 0) = +M_1^{eq}$ and $M_2(t = 0) = -M_2^{eq}$. With these boundary conditions, the constants in Eq. [2] become

$$C_1 = -C_2 = -2M_2^{eq}\sigma_{21}/(\lambda_1 - \lambda_2). \qquad [4]$$

The equilibrium initial state M_1^{eq} can be expressed as

$$M_1^{eq} = \frac{\gamma_1}{\gamma_2} M_2^{eq}. \qquad [5]$$

The Relaxation Matrix

The Solomon equations can easily be extended to more spins and solved using a matrix representation (*11, 12*). In order to follow the definition of equilibrium magnetization introduced in the Solomon equations and used above, we define the equilibrium magnetization as $\mathbf{M}^{eq}$. This is different from what has been commonly used in describing the NOESY experiment where it is defined as 0 (*11, 12*). The Solomon equation in matrix representation is

$$\frac{d\mathbf{M}}{dt} = -\mathbf{R} \cdot \Delta\mathbf{M}, \qquad [6]$$

where $\Delta\mathbf{M} = \mathbf{M} - \mathbf{M}^{eq}$ and the elements of the relaxation matrix $\mathbf{R}$ are

$$R_{ii} = \sum_j \rho_{ij} + \rho^*,$$

$$R_{ij} = \sigma_{ij} \qquad [7]$$

where ρ_{ij} and σ_{ij} are the individual auto- and cross-relaxation rates and ρ^* is a leakage term. The general solution for the vector of transient magnetizations $\mathbf{M}$, as a function of the mixing time t, is

$$\mathbf{M}(t) = \boldsymbol{\chi}^{-1} \cdot \Lambda \cdot \chi \cdot \Delta\mathbf{M}(t = 0) + \mathbf{M}^{eq}, \qquad [8]$$

where $\mathbf{\Lambda}$ is a diagonal matrix with the diagonal elements $e^{-\lambda_i t}$, and λ_i are the eigenvalues of the relaxation matrix $\mathbf{R}$. $\boldsymbol{\chi}$ is the matrix of eigenvectors of $\mathbf{R}$. $\Delta\mathbf{M}(t = 0)$ is the value of $\Delta\mathbf{M}$ after the initial pulse, which is the boundary condition. The individual auto- and cross-relaxation rate constants are given by

$$\rho_{ij} = \left(\frac{\mu_0}{4\pi}\right)^2 \frac{\gamma_i^2 \gamma_j^2 \hbar^2}{4r_{ij}^6} \times [6J(\omega_i + \omega_j) + 3J(\omega_i) + J(\omega_i - \omega_j)] \qquad [9]$$

$$\sigma_{ij} = \left(\frac{\mu_0}{4\pi}\right)^2 \frac{\gamma_i^2 \gamma_j^2 \hbar^2}{4r_{ij}^6} [6J(\omega_i + \omega_j) - J(\omega_i - \omega_j)]. \qquad [10]$$

The values of the constants used in Eqs. [9]–[10] are $\gamma_H = 26.752 \times 10^7$ rad s^{-1} T^{-1}, $\gamma_C = 6.728 \times 10^7$ rad s^{-1} T^{-1}, $\hbar = 1.0546 \times 10^{-34}$ Js, and $\mu_0 = 4\pi \times 10^{-7}$ TmA^{-1}.

Pulse Sequences

Cross relaxation rates were measured using the pulse sequence shown in Fig. 1. The pulse sequence starts with a nonselective or selective inversion of proton magnetization. After a variable mixing time *mix*, the magnetization is transferred to the *J*-coupled proton using sensitivity-enhanced coherence transfer (*13, 14*) of in-phase magnetization (*15, 16*) for detection. Pulsed field gradients can be used for coherence-order selection without sensitivity loss for superior water suppression (*17*). In order to suppress the spin diffusion (*18*), we also performed experiments using a modified pulse sequence similar to QUIET-NOESY (*7*). In the middle of the mixing time, both spins of the spin pair under

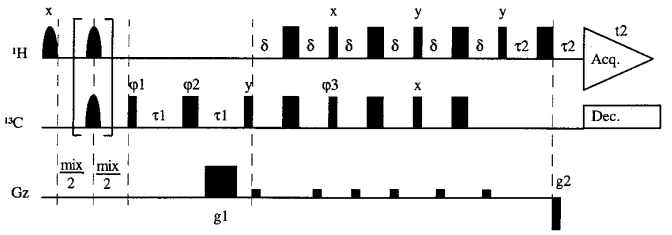

FIG. 1. The heteronuclear pulse sequence with sensitivity enhancement for selective measurement of transient Overhauser effects. Black thin and thick vertical bars represent 90° and 180° pulses, respectively. Shaped pulses are indicated with ellipsoid-shaped symbols. The gradients g1 and g2 were applied with a strength of 30 G/cm during 1.0 and 0.2541 ms, respectively. The delay δ was set to $1/(4J)$. The delays $\tau 1$ and $\tau 2$ were set to 1.37 and 0.5 ms, respectively. The phase is X when nothing else is stated. The phase cycle: $\varphi 1 = X, -X$; $\varphi 2 = X, X, -X, -X$; $\varphi 3 = Y, Y, -Y, -Y$; Acq. = $X, -X, -X, X$. The simultaneous selective-inversion pulses in the middle of the mixing period *mix*, shown in brackets, are used to suppress the effect of cross relaxation caused by other protons. The spectrum is in this case obtained by taking the difference between spectra recorded with and without the initial proton inversion pulse.

study are selectively inverted. Then the direct cross relaxation between the two nuclei under study can be measured as a difference between two experiments where one of the experiments starts with selective proton inversion and the other one without inversion. In this way, the effects of cross relaxation involving other nuclei could be effectively suppressed.

Model of Dynamics

The dynamics of the motilin molecule can be described by the model-free spectral-density function (*1, 2*)

$$J(\omega) = \frac{2}{5}\left[\frac{S^2\tau_M}{1 + (\omega\tau_M)^2} + \frac{(1 - S^2)\tau}{1 + (\omega\tau)^2}\right], \qquad [11]$$

where

$$\tau^{-1} = \tau_e^{-1} + \tau_M^{-1} \qquad [12]$$

with the generalized order parameter S^2, an overall rotational correlation time τ_M, and an effective internal correlation time τ_e.

EXPERIMENTAL

Sample Preparation

Motilin was synthesized with a single ^{13}C-enriched α carbon in the leucine at position 10 (*9*). Porcine motilin has the sequence $FVPIF_5TYGEL_{10}QRMQE_{15}KERNK_{20}GQ$ and a molecular mass of 2698 Da with a single ^{13}C label. The NMR sample was prepared by dissolving 12.7 mg of lyophilized peptide in 600 μl of 60% (v/v) H_2O, 10% (v/v) D_2O, and 30% (v/v) deuterated 1,1,1,3,3,3-hexafluoro-2-propanol. Twenty millimolar deuterated acetic acid was used as buffer and the pH 3.9 was adjusted using minute amounts of solid NH_4HCO_3. The sodium salt of 3-trimethylsilyl-[3,3,2,2-D]-propionic acid was used as an internal chemical-shift reference (0.2 m*M*). The peptide concentration was 7.1 m*M*, estimated using the molar extinction coefficient of tyrosine $\epsilon_{274.6\,nm} = 1420\ M^{-1}\ cm^{-1}$ (*19*).

NMR Spectroscopy

All experiments were run at 35°C using Varian Unity or Unity*plus* spectrometers operating at 600 MHz proton frequency. The proton and carbon 90° pulse widths were about 6 and 18 μs, respectively. The spectra were recorded with a 6 kHz spectral window. The proton frequency was centered on the water signal and the carbon frequency was set on resonance on the frequency of the ^{13}C label. The proton selective pulses used were 7 ms long and of I-BURP-1 (*20*) type, centered at 2.6, 4.2, and 7.5 ppm for β, α, and NH protons, respectively. Control experiments in order to check off-resonance effects were run with the selective pulse centered at 0.0 ppm. A recycle delay of 5 s was used and a total of 128 transients was acquired for each variable delay time *mix*. The list of *mix* used in the cross-relaxation experiments was 0, 0.05, 0.1, 0.15, 0.2, 0.25, 0.3, 0.35, 0.4, 0.45, 0.5, 0.6, 0.7, 0.8, 0.9, 1.0, 1.1, 1.2, 1.3, 1.4, 1.5, 1.7, 1.9, 2.1, 2.3, 2.5, 3.0, 3.5, 4.0, 4.5, and 5.0 s. Each series of experiments, with 31 values of the delay time *mix*, took about 6 h. Spectra were acquired using 83 ms acquisition time, multiplied with a 5 Hz exponential line broadening, and Fourier transformed into 8192-point frequency-domain spectra. The transient NOE curves were fitted using the program gnuplot v.3.6 (*21*), and reported errors of time constants corresponding to a 68.3% confidence interval.

The relaxation-matrix calculations were performed using Mathematica (*22*) software. The relaxation-matrix program was rewritten for heteronuclear spin systems and model-free spectral-density functions, based on an earlier program generously provided by Dr. J. Shriver.

RESULT AND DISCUSSION

The pulse sequence presented in Fig. 1 was used in order to measure heteronuclear cross-relaxation rates in the sample of motilin with a ^{13}C label at the α carbon of Leu^{10}. The transient magnetization curves of nonselective and selective experiments are shown in Fig. 2. The transient magnetization curves were analyzed using the Solomon equations for a two-spin system and the results are shown in Table 1.

Nonselective Inversion of All Protons

The cross relaxation rate, measured by nonselective inversion of all protons is $0.15 \pm 0.003\ s^{-1}$ as seen in Table 1 and

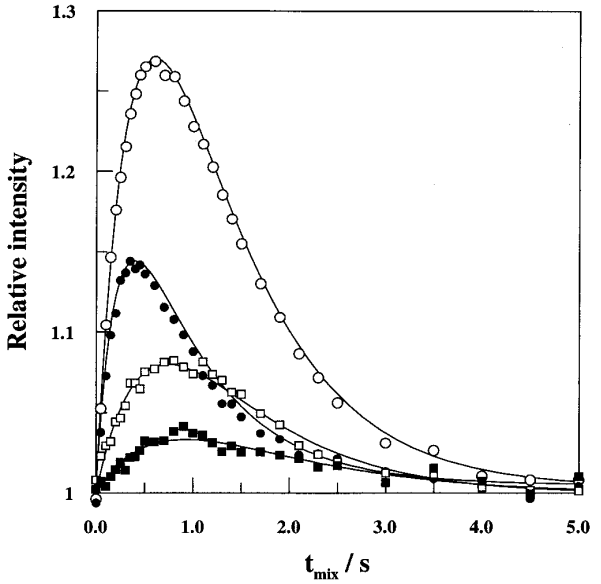

FIG. 2. Transient curves of ^{13}C magnetization after nonselective inversion of all protons (open circles), after selective inversion of α protons (filled circles), after selective inversion of β protons (open squares), and after selective inversion of NH protons (filled squares). The apparent cross-relaxation rates obtained from a fitting of the Solomon equations using a two-spin approximation are nonselective $\sigma(H^{all} \rightarrow C^{\alpha}) = 0.15 \pm 0.003\ s^{-1}$, selective $\sigma(H^{\alpha} \rightarrow C^{\alpha}) = 0.13 \pm 0.006\ s^{-1}$, $\sigma(H^{\beta} \rightarrow C^{\alpha}) = 0.033 \pm 0.001\ s^{-1}$, and $\sigma(H^{N} \rightarrow C^{\alpha}) = 0.013 \pm 0.002\ s^{-1}$. It should be noted that the cross-relaxation rates measured between the α carbon and the β protons or NH proton are spin diffusion limited and not direct rates.

is in reasonably good agreement with the cross-relaxation rate $\sigma_{SS} = 0.17 \pm 0.02\ s^{-1}$, calculated from the steady-state $\{^1H\}-^{13}C$ NOE and the ^{13}C T_1 (*8*). The carbon and the nonselective proton longitudinal-relaxation rates obtained from the fitting are also close to the directly measured rates.

Selective Inversion

We performed selective experiments where we used selective pulses in order to separate the cross-relaxation rates from different protons. The incomplete inversion when using a selective pulse can be taken into account by introducing an inversion coefficient into Eq. [4] instead of a constant value of 2, which is the value for ideal inversion. We observed that the intensity of the part of a spectrum inverted using a 7 ms I-BURP-1 pulse was 90% compared with the intensity of the same part of a spectrum observed without selective inversion. The 90% inversion corresponds to a inversion coefficient of 1.9. The experimental transients were analysed using Eqs. [2]–[5], and the time constants from the nonselective and the three selective experiments are listed in Table 1. The use of an inversion coefficient in order to account for the incomplete inversion directly affected the measured values of the cross-relaxation rates. It should be noted that some cross relaxation will also occur during the time that the selective pulse is applied. The effect should be small in our case since the length of the selective pulse is much shorter than the time corresponding to the cross-relaxation rates we are measuring. This problem may be avoided by using the approach by Kessler *et al.* (*23*, *24*), if relaxation during the selective pulse cannot be neglected.

The cross-relaxation rate, measured by selective inversion of the α proton, was $0.13 \pm 0.006\ s^{-1}$ as seen in Table 1 and is somewhat slower than the cross-relaxation rate determined from nonselective inversion. This could be expected if the contributions from other protons are not negligible. The carbon and the selective-proton longitudinal-relaxation rate obtained from the fitting are however not close to the directly measured rates, see Table 1.

For β protons and the NH proton (Fig. 2), the two-spin model used for fitting rates is oversimplified. Although the selective cross-relaxation rates reported in the legend of Fig. 2 for β and NH protons are smaller than the α-proton cross-relaxation rate, we do not consider these rates to be direct cross-relaxation rates. They should rather be regarded as secondary rates mediated by spin diffusion via the α proton.

In order to have a more realistic model for β and NH

TABLE 1
Relaxation Rates Describing the $^{13}C^{\alpha}-^{1}H^{\alpha}$ Vector Dynamics of Leu[10] in the 22 Residue Peptide Hormone Motilin

Experiment	σ_{CH} (s^{-1})	R_C (s^{-1})	$R_H^{(sel)}$ (s^{-1})	$R_H^{(ns)}$ (s^{-1})
Separate experiments[a]: ^{13}C T_1, ^{1}H T_1 $^{(sel)}$, ^{1}H T_1 $^{(ns)}$, and $\{^1H\}-^{13}C$ NOE	0.17 ± 0.02	2.30 ± 0.02	3.30 ± 0.01	1.22 ± 0.01
Nonselective proton inversion	0.15 ± 0.003	2.34 ± 0.1	—	1.14 ± 0.06
Selective α-proton inversion	0.13 ± 0.006	4.49 ± 0.4	1.24 ± 0.1	—
Selective α-proton inversion with suppression of spin diffusion	0.13 ± 0.006[b]	2.0 ± 1.0[b]	3.3 ± 1.0[b]	—
	0.13 ± 0.003[c]	2.30[c]	3.1 ± 0.1[c]	—

Note. The cross- and longitudinal-relaxation rates were obtained from the transient magnetization curves using the two-spin approximation for the Solomon equations. σ_{CH} is the heteronuclear cross-relaxation rate, R_C is the ^{13}C longitudinal-relaxation rate, and $R_H^{(sel)}$ and $R_H^{(ns)}$ are the selective and nonselective ^{1}H longitudinal-relaxation rates, respectively.

[a] Data from (*8*).

[b] From a three-parameter fit to the Solomon equations.

[c] From a two-parameter fit with the carbon longitudinal-relaxation rate (R_C) used as a constant determined from an independent experiment.

TABLE 2

The Internuclear Distances r_{ij} in Angstroms, Used to Calculate Transient Magnetization Using the Relaxation-Matrix Approach, as Derived from the Previously NMR-Determined Structure of Motilin (*25*)

	C^{α}	NH	H^{α}	$H^{\beta 1}$
$H^{\beta 2}$	2.11	3.50	2.31	1.76
$H^{\beta 1}$	2.15	3.90	2.50	
H^{α}	1.09	2.92		
NH	2.105			

proton cross relaxation with the α carbon, we simulated a five-spin system using the relaxation-matrix approach. We included in the simulation the spin-$\frac{1}{2}$ nuclei of the leucine residue that are close to the ^{13}C-labeled α carbon, i.e., the α proton, the two β protons, and the NH proton. The atomic co-ordinates used in the calculations were taken from the NMR-determined structure of motilin (*25*) and the distances used in the calculations are listed in Table 2. Incomplete inversion of resonances is taken care of in the simulations by setting the elements of the boundary-condition vector $\Delta\mathbf{M}(t = 0)$ in Eq. [8] equal to $-2M_{\mathrm{H}}^{\mathrm{eq}}$ for ideal inversion and $-1.9\ M_{\mathrm{H}}^{\mathrm{eq}}$ in the case of inversion by a selective pulse. The leakage term ρ^* in Eq. [7] is applied only for protons. The leakage rate was assigned the value 1 s^{-1} (*26*). This additional rate will account for the relaxation caused by more distant protons. The numerical values of the model-free spectral-density function parameters used were $\tau_{\mathrm{M}} = 2.95$ ns, $\tau_{\mathrm{e}} = 68$ ps, and $S^2 = 0.87$. These values had given the best fit to the measured α-carbon T_1, T_2, and steady-state $\{^1\mathrm{H}\} - ^{13}\mathrm{C}$ NOE (*8*). The structural parameters in Table 2 together with the dynamic data were used to calculate the theoretical cross-relaxation rates shown in Table 3.

It is extremely complicated to get a more accurate estimate for the contribution of distant protons, as they may also experience different kinds of dynamics. For example, the methyl protons have a completely different spectral-density function, and even the proton–proton distance is time dependent.

TABLE 3

The Cross-Relaxation Rates (S^{-1}) of the Five-Spin System, Calculated Using Eqs. [6]–[12]

	C^{α}	NH	H^{α}	$H^{\beta 1}$
$H^{\beta 2}$	0.003	−0.078	−0.94	−4.8
$H^{\beta 1}$	0.003	−0.041	−0.58	
H^{α}	0.18	−0.23		
NH	0.003			

Note. The dynamics of the molecule was described by a model-free spectral-density function with the parameters $\tau_{\mathrm{M}} = 2.95$ ns, $\tau_{\mathrm{e}} = 69$ ps, and $S^2 = 0.87$ (*8*). The internuclear distances used in the calculation are listed in Table 2.

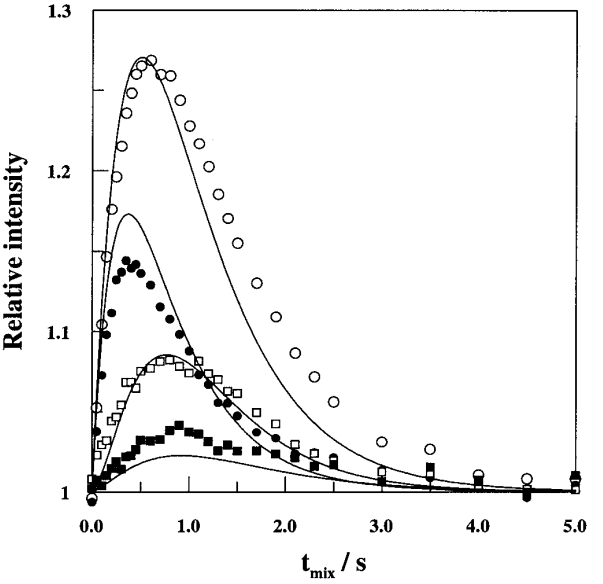

FIG. 3. Simulation of the transient magnetization curves using relaxation-matrix calculations on a five-spin system and the corresponding experimental results taken from Fig. 2. The five-spin system consists of the α proton, the two β-protons, the NH proton, and the α carbon. The internuclear distances used in the simulation are listed in Table 2 and the cross-relaxation rates are listed in Table 3.

The comparison between experimental data and simulation using the five-spin system with the cross-relaxation rates shown in Table 3 is presented in Fig. 3. These results show rather good qualitative agreement between experiment and simulation. The differences between the real and simulated curves are mainly due to the limited size of the simulated system and the coarse approximation that all vectors can be described by the same set of dynamic parameters. The difference between simulated and real transient magnetization for the nonselective inversion is probably due to the fact that neighboring protons with slow longitudinal relaxation rates supply the α carbon with magnetization during long mixing times. The observed differences for the corresponding selective experiment is mostly dependent on the fact that we have used the faster cross-relaxation rate calculated from the steady-state $\{^1\mathrm{H}\} - ^{13}\mathrm{C}$ NOE and $^{13}\mathrm{C}$ T_1 (*8*) in the simulation rather than that measured using transient methods.

Quenching of Spin Diffusion

If one wants to use quantitative rates, the spin system must be simplified further as it is not possible to model the contribution from other spins with the accuracy needed for

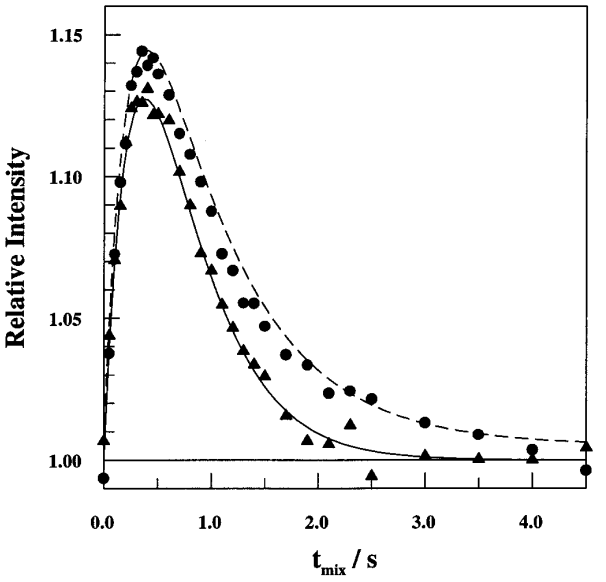

FIG. 4. Transient ^{13}C magnetization curves after a selective inversion of the α-proton magnetization with (filled triangles) and without suppression of spin diffusion (filled circles). When suppressing the spin diffusion, the α-proton and α-carbon magnetization is selectively inverted in the middle of the mixing time. The data with suppression of spin diffusion (filled triangles) represent the difference of two experiments, using the pulse sequence shown in Fig. 1, where one of the experiments starts with a selective proton inversion. The curves are obtained from fitting of the Solomon equations using a two-spin approximation, and the relaxation rates obtained are presented in Table 1.

quantification. In order to further simplify the spin system under study, we used a modified pulse sequence similar to QUIET-NOESY (*7*), as described under Theory. The cross relaxation from the α proton to other protons could in this way be effectively suppressed by using an experiment involving selective inversion of α-proton and α-carbon magnetization in the middle of the mixing time.

The resulting transient magnetization curve is shown in Fig. 4. For comparison, the corresponding curve without suppression of spin diffusion is also shown. It is obvious that suppression of spin diffusion significantly accelerates the return to equilibrium. The heteronuclear cross-relaxation rate between the α carbon and α proton measured using spin-diffusion suppression was $0.13 \pm 0.006\ s^{-1}$ (Table 1). The main difference in the results from experiments of selective α-proton inversion with and without suppression of spin diffusion appears in the longitudinal ^{13}C and ^{1}H relaxation rates. The longitudinal-relaxation rates measured by the selective experiment with suppression of spin diffusion were 2.0 ± 1.0 and $3.3 \pm 1.0\ s^{-1}$. These values agree well with α-carbon and α-proton selective longitudinal-relaxation rates measured separately.

The long recycle delay, needed for cross-relaxation rate experiments, has been one of the major limiting factors in getting accurate cross-relaxation rates. Now, using spin-diffusion suppression, the system returns to equilibrium with the fast selective α-proton longitudinal-relaxation rate (Fig. 4). This allows the advantage of using shorter recycle delays in the experiments.

The technique used here to decouple the cross relaxation to other protons makes it, in principle, possible to measure longitudinal-relaxation rates of the heteronucleus and the proton as well as their cross-relaxation rate from a single experiment. As seen in Table 1, a three-parameter fit to the experiment gives reasonable values of the rates but with relatively large uncertainties. Alternatively, if the ^{13}C longitudinal-relaxation rate is measured separately, a two-parameter fit gives values with smaller uncertainties (Table 1). This strategy could be useful in order to measure, in a single additional experiment, the cross-relaxation rate and the proton selective-relaxation rate, both of which are needed for spectral-density mapping.

CONCLUSIONS

We have described a selective transient experiment to directly measure the NMR cross-relaxation rate of a *J*-coupled heteronucleus–proton pair. The sensitivity of this experiment is enhanced by proton detection and could therefore be applied to samples of millimolar concentration. The water signal is suppressed using coherence selection by magnetic field gradient pulses. The experiment can easily be extended into a two-dimensional version, where the sensitivity-enhancement technique can be applied to recover the loss of sensitivity which otherwise might accompany the gradient selection.

In comparison with Solomon's original study of spin dynamics of neat HF (*4*), we are now able to study four orders of magnitude less-concentrated samples and to selectively remove the cross relaxation from neighboring nuclei. Due to effective suppression of spin diffusion, short recycle delays are possible. The selectivity of measured rates makes this experiment useful for the study of molecular mobility.

The evaluated cross-relaxation rates in the heteronuclear pair measured using the traditional heteronuclear steady-state NOE and the selective experiment described here are in reasonably good agreement.

ACKNOWLEDGMENTS

We thank Professor A. Ehrenberg for valuable discussions. We also thank the Swedish NMR Center for the use of the Varian UNITY 600 MHz spectrometer. The Swedish NMR centre staff Charlotta Damberg and Lotta Johansson are thanked for skillful help. A fellowship to J.J. from the Wenner-Gren Center Foundation is gratefully acknowledged. This work was supported by grants from the Swedish Natural Science Research Council.

REFERENCES

1. G. Lipari and A. Szabo, *J. Am. Chem. Soc.* **104,** 4546–4559 (1982).
2. G. Lipari and A. Szabo, *J. Am. Chem. Soc.* **104,** 4559–4570 (1982).
3. J. W. Peng and G. Wagner, *J. Magn. Reson.* **98,** 308–332 (1992).
4. I. Solomon, *Phys. Rev.* **99,** 559–565 (1955).
5. J. Fejzo, W. M. Westler, S. Macura, and J. L. Markley, *J. Magn. Reson.* **92,** 195–202 (1991).
6. J. Fejzo, W. M. Westler, J. L. Markley, and S. Macura, *J. Am. Chem. Soc.* **114,** 1523–1524 (1992).
7. C. Zwahlen, S. J. F. Vincent, L. Di Bari, M. H. Levitt, and G. Bodenhausen, *J. Am. Chem. Soc.* **116,** 362–368 (1994).
8. J. Jarvet, P. Allard, A. Ehrenberg, and A. Gräslund, *J. Magn. Reson. B* **111,** 23–30 (1996).
9. P. Allard, J. Jarvet, A. Ehrenberg, and A. Gräslund, *J. Biomol. NMR* **5,** 133–146 (1995).
10. J. H. Noggle and R. E. Schirmer, ''The Nuclear Overhauser Effect,'' Academic Press, New York, 1971.
11. J. W. Keepers and T. L. James, *J. Magn. Reson.* **57,** 404–426 (1984).
12. W. Massefski and P. H. Bolton, *J. Magn. Reson.* **65,** 526–530 (1985).
13. J. Cavanagh and M. Rance, *J. Magn. Reson.* **88,** 72–85 (1990).
14. J. Cavanagh, A. G. Palmer III, P. E. Wright, and M. Rance, *J. Magn. Reson.* **91,** 429–436 (1991).
15. J. Schleucher, M. Schwendinger, M. Sattler, P. Schmidt, O. Schedletzky, S. J. Glaser, O. W. Sørensen, and C. Griesinger, *J. Biomol. NMR* **4,** 301–306 (1994).
16. K. T. Dayie and G. Wagner, *J. Magn. Reson. A* **111,** 121–126 (1994).
17. L. E. Kay, P. Keifer, and T. Saarinen, *J. Am. Chem. Soc.* **114,** 10,663–10,665 (1992).
18. A. Kalk and H. J. C. Berendsen, *J. Magn. Reson.* **24,** 343–366 (1976).
19. D. B. Wetlaufer, *Adv. Protein Chem.* **17,** 303–390 (1962).
20. H. Geen and R. Freeman, *J. Magn. Reson.* **93,** 93–141 (1991).
21. T. Williams and C. Kelley, ''gnuplot: An Interactive Plotting Program,'' 1996.
22. S. Wolfram, ''Mathematica: A System for Doing Mathematics by Computer,'' Addison–Wesley, New York, 1991.
23. H. Kessler, H. Oschkinat, C. Griesinger, and W. Bermel, *J. Magn. Reson.* **70,** 106–133 (1986).
24. H. Kessler, U. Anders, G. Gemmecker, and S. Steuernagel, *J. Magn. Reson.* **85,** 1–14 (1989).
25. S. Edmondson, N. Khan, J. Shriver, J. Zdunek, and A. Gräslund, *Biochemistry* **30,** 11,271–11,279 (1991).
26. G. M. Clore and A. M. Gronenborn, *J. Magn. Reson.* **84,** 398–409 (1989).